



# 1 Towards agricultural soil carbon monitoring, reporting and 2 verification through Field Observatory Network (FiON)

3 Olli Nevalainen<sup>1</sup>, Olli Niemitalo<sup>2</sup>, Istem Fer<sup>1</sup>, Antti Juntunen<sup>2</sup>, Tuomas Mattila<sup>3</sup>, Olli Koskela<sup>2</sup>, Joni  
4 Kukkamäki<sup>2</sup>, Layla Höckerstedt<sup>1</sup>, Laura Mäkelä<sup>4</sup>, Pieta Jarva<sup>4</sup>, Laura Heimsch<sup>1</sup>, Henriikka Vekuri<sup>1</sup>, Liisa  
5 Kulmala<sup>1,5</sup>, Åsa Stam<sup>1</sup>, Otto Kuusela<sup>1,6,7</sup>, Stephanie Gerin<sup>1</sup>, Toni Viskari<sup>1</sup>, Julius Vira<sup>1</sup>, Jari Hyväluoma<sup>2</sup>,  
6 Juha-Pekka Tuovinen<sup>1</sup>, Annalea Lohila<sup>1,6</sup>, Tuomas Laurila<sup>1</sup>, Jussi Heinonsalo<sup>5</sup>, Tuula Aalto<sup>1</sup>, Iivari  
7 Kunttu<sup>2</sup>, Jari Liski<sup>1</sup>

8

9 <sup>1</sup> Finnish Meteorological Institute, FMI, Helsinki, Finland

10 <sup>2</sup> Häme University of Applied Sciences, HAMK, Hämeenlinna, Finland

11 <sup>3</sup> Finnish Environment Institute, SYKE, Helsinki, Finland

12 <sup>4</sup> Baltic Sea Action Group, BSAG, Espoo, Finland

13 <sup>5</sup> University of Helsinki, Institute for atmospheric and Earth system research (INAR), forest sciences, Helsinki, Finland

14 <sup>6</sup> University of Helsinki, Institute for atmospheric and Earth system research (INAR), physics, Helsinki, Finland

15 <sup>7</sup> University of Amsterdam, Computational Science, Amsterdam, Netherlands

16

17 *Correspondence to:* (olli.nevalainen@fmi.fi)

18 **Abstract.** Better monitoring, reporting and verification (MRV) of the amount, additionality and persistence of the sequestered  
19 soil carbon is needed to understand the best carbon farming practices for different soils and climate conditions, as well as their  
20 actual climate benefits or cost-efficiency in mitigating greenhouse gas emissions. This paper presents our Field Observatory  
21 Network (FiON) of researchers, farmers, companies and other stakeholders developing carbon farming practices. FiON has  
22 established a unified methodology towards monitoring and forecasting agricultural carbon sequestration by combining offline  
23 and near real-time field measurements, weather data, satellite imagery, modeling and computing networks. FiON's first phase  
24 consists of two intensive research sites and 20 voluntary pilot farms testing carbon farming practices in Finland. To disseminate  
25 the data, FiON built a web-based dashboard called Field Observatory (v1.0, fieldobservatory.org). Field Observatory is  
26 designed as an online service for near real-time model-data synthesis, forecasting and decision support for the farmers who are  
27 able to monitor the effects of carbon farming practices. The most advanced features of the Field Observatory are visible on the  
28 Qvidja site which acts as a prototype for the most recent implementations. Overall, FiON aims to create new knowledge on  
29 agricultural soil carbon sequestration and effects of carbon farming practices, and provide an MRV tool for decision-support.

30



## 31 **1 Introduction**

32 Farmers are managing one of the largest carbon stocks on the planet where even relatively small additions are important for  
33 climate change mitigation. Accordingly, the international “soil carbon 4 per mille” initiative aims at raising the soil organic  
34 carbon content by 0.4 % per year by adopting carbon farming practices (Minasny et al. 2017). Carbon farming practices include  
35 methods, such as reduced soil disturbance (reduced or zero tillage), increasing carbon inputs (soil amendments, cover crops,  
36 residue management) and crop rotations. Such practices do not only have the potential to partially refill the global soil carbon  
37 stock that has lost 116 Pg carbon due to land cultivation (Sanderman et al., 2017), but they could also improve soil structure  
38 and health, and increase crop yields (Merante et al. 2017; Oldfield et al. 2018). Annual carbon sequestration rates for different  
39 management practices vary from 100 to 1000 kg C ha<sup>-1</sup> (Merante et al., 2017; Minasny et al., 2017). Detecting sequestration  
40 rates in this range is difficult with traditional empirical soil sampling designs due to large spatial variability of soil carbon  
41 content and small relative changes in the soil carbon stock due to individual management actions (VandenBygaert and Angers  
42 2006; Heikkinen et al. 2021). This calls for better monitoring, reporting and verification (MRV) of the amount, additionality  
43 and persistence of the sequestered soil carbon due to carbon farming practices.

44  
45 Towards this goal, we established the Field Observatory Network (FiON), a network of researchers, farmers, companies and  
46 other stakeholders applying carbon farming practices. FiON has created a unified methodology to monitor and forecast  
47 agricultural carbon sequestration, by combining automated near real-time field measurements, weather data, satellite imagery,  
48 modeling and computing networks. In general, FiON follows the principles of other ecological observatory networks, such as  
49 National Ecological Observatory Network (NEON, Keller et al., 2008), Global Lake Ecological Observatory Network  
50 (GLEON, Hipsey et al., 2017) and Biodiversity Observatory Networks (GEOBON, Guerra et al., 2021) that collect long-term  
51 ecological data and monitor the effects of climate and land use change (Elmendorf 2016; Hinckley et al., 2016; Hipsey et al.,  
52 2017; Keller et al., 2008). The primary purpose of FiON, however, is to i) create new knowledge on soil processes, ii) to  
53 measure, verify and forecast the carbon sequestration in agricultural soils and to iii) approximate the effects of carbon farming  
54 practices on yield, biomass and CO<sub>2</sub> flux in near real-time. To achieve this, FiON invested in the use and development of a  
55 community cyberinfrastructure tool, Predictive Ecosystem Analyzer (PEcAn, pecanproject.org), which enables synthesizing  
56 different data sources and process-based models, quantifying and partitioning uncertainties, and operationalizing near real-  
57 time ecological forecasting (Fer et al., 2021). To disseminate the observations and findings, we built a free-access online  
58 dashboard called Field Observatory (v1.0, fieldobservatory.org). This website serves as a tool to monitor the impacts of carbon  
59 farming practices. The dashboard integrates data from field sensors, remote sensing and field survey. In this sense, FiON will  
60 provide decision support for the farmers, at first hand via the Field Observatory website and in due course via the scientific  
61 synthesis informed by the best available data and models. To serve the research and other interested communities, the data in  
62 Field Observatory is publicly available and downloadable from the website.

63



64 In this paper our objectives are to 1) describe data flows from various manual and automatic measurements in the Field  
65 observatory, 2) demonstrate 15-day forecasts of carbon exchange and plant growth towards decision support for the farmers,  
66 and 3) discuss the benefits of the public monitoring network established by FiON.

67  
68 First, we introduce the sites included in FiON, and describe the tested carbon farming practices. Next, we describe the FiON  
69 workflow from data collection, processing and storage to visualization and dissemination through the Field Observatory  
70 website. Finally, we present the near real-time model-data synthesis, forecasting and decision support for the users.

## 71 **2 Sites and tested carbon farming practices**

72 The first phase of FiON consists of two intensive agricultural research sites and 20 voluntary farms testing carbon farming  
73 practices (Fig. 1, <https://www.fieldobservatory.org/MapView>). These 20 farms, called Advanced Carbon Action farms (ACA),  
74 were selected out of 100 pilot farms participating in the Carbon Action platform<sup>1</sup>, where volunteer farmers test carbon farming  
75 practices (Mattila et al. 2021). Each farm has a test field and an adjacent, conventionally managed, control field (field 1 and 0  
76 in Field Observatory, respectively). The additional carbon farming practices aim to increase carbon sequestration through  
77 increasing photosynthesis, exogenous inputs or through decreasing decomposition (Minasny et al., 2017). These practices  
78 (Table 1) are: cover crops, adaptive grazing, soil amendments, subsoiling and ley farming (introducing a grass crop into  
79 rotation). Each farmer made a five-year carbon farming plan and took soil samples at the beginning of the study from GPS  
80 located points in the field. The same points are monitored annually and also contain real-time soil sensors.

81

---

<sup>1</sup>

Carbon Action platform consists of several scientific projects, 100 farms committed to 5 years of research activity and farmer extension services. As of spring 2021, some 600 farmers are participating around the topic. Food system companies and organisations are also involved. Carbon Action is led by BSAG and the research is coordinated by FMI. More <https://carbonaction.org/en/front-page/>



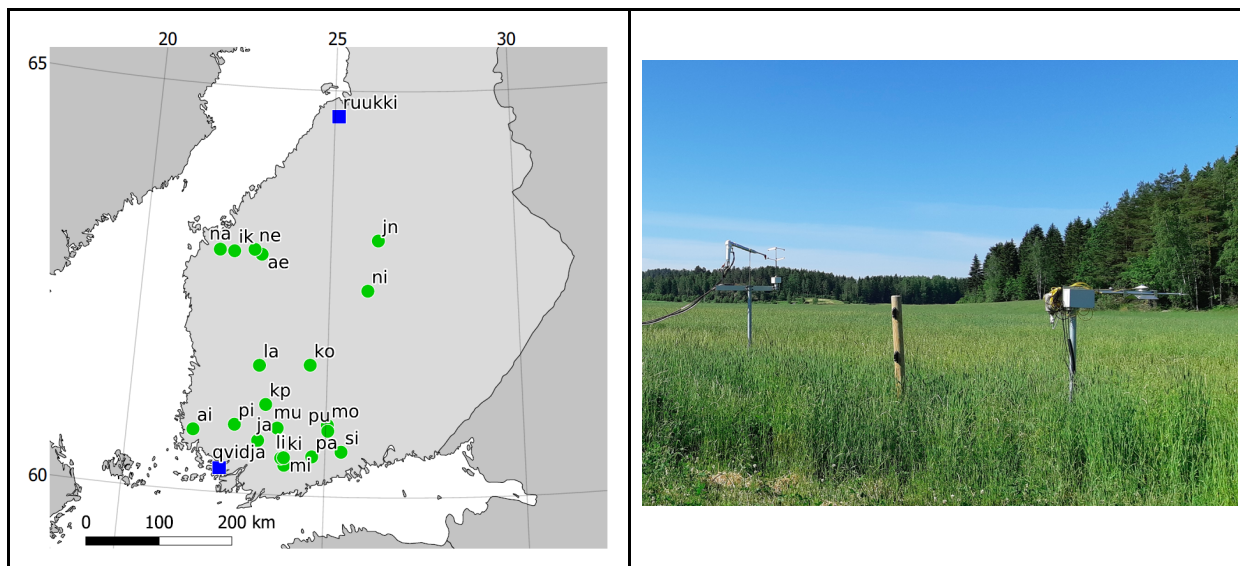
82

83 **Table 1 Principles of the carbon farming practices tested at the Carbon Action farms.**

Carbon farming practice	Principles for carbon sequestration
Cover crops	Crops planted to lengthen photosynthetically active period and to increase carbon assimilation, carbon and root inputs and to reduce leaching of carbon and nutrients.
Adaptive grazing	Short grazing & long rest periods to manage grass growth for increased root growth and increased soil cover.
Soil amendments	Exogenous carbon input. In addition may stimulate plant growth through increased water holding capacity, nutrients, etc.
Subsoiling	Removing physical barriers to root growth by soil loosening. Coupled to a grass crop to stabilize loosened soil. Increases plant growth and soil aeration and decreases bulk density.
Ley farming	Breaking monocropping with perennial grass. Increases photosynthesis, root input and diversity.
Grass cultivation	Diverse plant species composition, increased cutting height and organic fertilization.

84

85 The 20 ACA farms were selected based on their chosen practice (four farms per measure), location (appropriate distances for  
86 survey work and even spread over Finnish farmland) and soil type (a mix of clay and sandy soils) (Table 2). All of them were  
87 included in a soil condition survey in 2019 (Mattila, 2020). Farms with anomalous measurements or too large organic matter  
88 content or nutrient differences between the control and treatment plots in the initial phase of FiON were excluded from ACA  
89 farms. FiON includes two intensive research sites, Qvidja and Ruuukki, which are operated by the Finnish Meteorological  
90 Institute (FMI). In Qvidja, carbon farming practices are tested in three different fields. In Ruukki, there are no carbon farming  
91 practices implemented at the moment. Both sites have eddy covariance towers which continuously monitor greenhouse gas  
92 fluxes and weather(see Sect. 3).



93

94 **Figure 1** Map of Advanced Carbon Action sites (green dots) and intensive sites (blue squares) (left), and eddy covariance  
 95 tower and radiation measurement instrumentation at Qvidja (right).

96

97 **Table 2** Current FiON sites.

Site	Site type	Soil type	Carbon farming practice	Species in 2020	Nearest FMI weather station
AE	ACA	Sandy loam	Subsoiling	Rye	Kauhava airport
KO	ACA	Silt	Subsoiling	Silage grass	Juupajoki Hyytiälä
KP	ACA	Clay loam	Subsoiling	Multi-species ley	Pirkkala airport
LA	ACA	Clay silt	Subsoiling	Oats	Pirkkala airport
JN	ACA	Fine sand	Adaptive grazing	Pasture grass	Vesanto Sonkari
MI	ACA	Clay loam	Adaptive grazing	Pasture grass	Lohja Porla
NI	ACA	Sand till	Adaptive grazing	Pasture grass	Jyväskylä airport AWOS
KI	ACA	Fine sand	Soil amendments	Multi-species ley	Somero Salkola
LI	ACA	Clay loam	Soil amendments	Spring wheat	Lohja Porla
PA	ACA	Clay loam	Soil amendments	Hay grass	Nurmijärvi Röykkä



PI	ACA	Clay loam	Soil amendments	Oats	Kaarina Yltöinen
MU	ACA	Clay loam	Grass mixture	Multi-species ley	Somero Salkola
NA	ACA	Loam	Cover crops	Peas	Vaasa airport
NE	ACA	Loam	Cover crops	Oats	Kauhava airport
PU	ACA	Silty clay loam	Cover crops	Oats	Mäntsälä Hirvihaara
SI	ACA	Clay loam	Cover crops	Multi-species ley	Porvoo Harabacka
AI	ACA	Silty clay	Ley farming	Multi-species ley	Rauma Pyympää
JA	ACA	Clay loam	Ley farming	Multi-species ley	Jokioinen Ilmala
IK	ACA	Sand till	Ley farming	Silage grass	Seinäjäki Pelmaa
MO	ACA	Loam	Ley farming	Barley	Hämeenlinna Lammi Pappila
Qvidja	Intensive	Clay loam	Grass cultivation	Silage grass	Kaarina Yltöinen*
Ruukki	Intensive	Organic (peat)	-	Silage grass	Siikajoki Ruukki*

98 \*Intensive sites have their own micrometeorological measurements.

99

### 00 3 Data collection

01 FiON combines multiple online and offline data streams with different temporal frequencies and geographical extent (Fig. 2,  
 02 Table 3). These data streams flow into a server where the data are pre-processed (filtered, gap-filled, formatted) and model-  
 03 data analyses are performed through an ecological cyberinfrastructure Predictive Ecosystem Analyzer (PEcAn, Fer et al.,  
 04 2021). All observational and computational outputs are stored in the server and disseminated through a web-based user  
 05 interface. In the following sections we describe each data stream and model-data activity in the order given in Fig. 2.

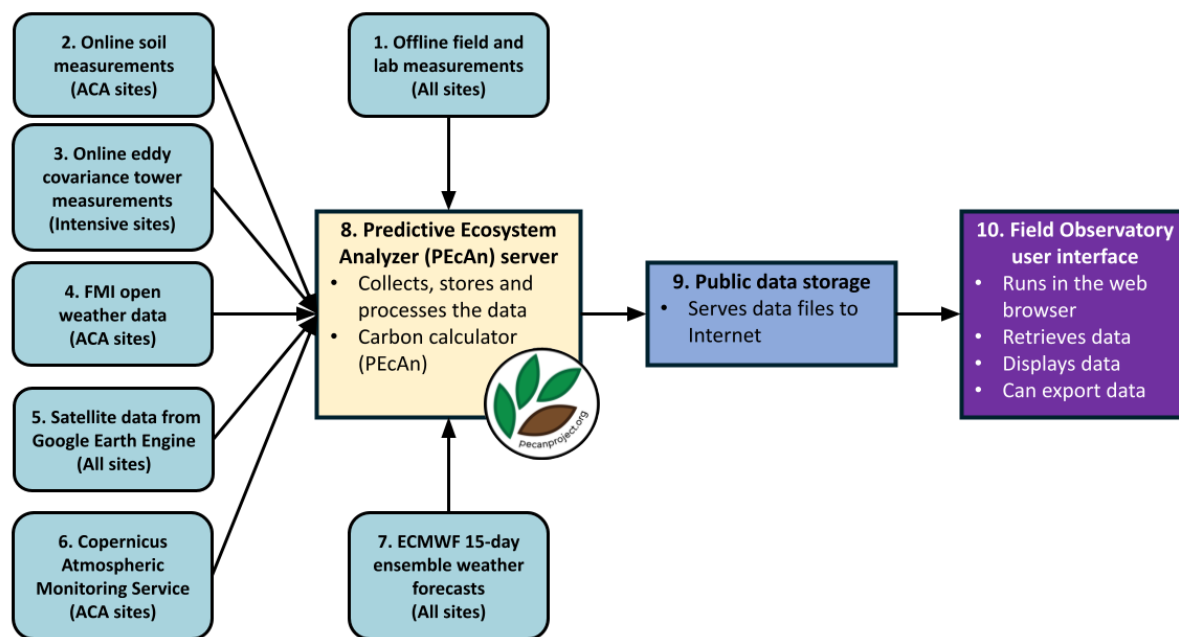


Figure 2 Overview of the FiON data flows.

06  
07  
08

### 09 3.1 Offline field and lab measurements

10 At ACA sites, the measurements are done at three, static measurement points per field. The points have c.a. 30-100 m distance  
11 from each other and are located on a transect line. They were located to cover the variability of the field and cover similar soil  
12 conditions in both the test and control plots. Annual soil sampling and soil quality measurements are made within a ten-meter  
13 radius of these points. All offline data from ACA sites on soil properties (cation exchange capacity, pH, organic matter),  
14 nutrients (P, K, S, Ca, Mg, Cu, Zn, B, Mn, Fe, Al, P-saturation), soil physical quality (soil structure, bulk density, porosity,  
15 water holding capacity, infiltration rate) and biological properties (earthworm counts, above ground biomass, percentage plant  
16 cover) are presented in Zenodo data repository with annual updates (Mattila, 2020; Mattila and Heinonen, 2021). The offline  
17 field measurements at the intensive site Quidja are described in Heimsch et al. (2021). Such offline, non-automated and  
18 infrequent data are currently being curated further for harmonization and reporting in JavaScript Object Notation (JSON) file  
19 formats and International Consortium for Agricultural Systems Applications (ICASA) standards (White et al., 2013). An  
20 example soil carbon measurement data point ( $16.59 \pm 2.25 \text{ kg m}^{-2}$ , average±standard deviation) is visualized on Quidja graphs  
21 and available on the accompanying JSON file (<https://data.lit.fmi.fi/field-observatory/qvidja/ec/events.json>).



### 22 3.1.1 Field activity

23 All field activity information (e.g. planting, fertilization, harvest timing and amount) is currently received offline through  
24 personal communication. An online application is under development for i) harmonizing historical field data, and for ii)  
25 collecting future field activity data. Accordingly, the application is being developed to allow the farmers themselves to enter  
26 these events and related details, and it will be tested for the first time at the end of the 2021 season. The application is written  
27 using the Shiny R package (v1.6.0, Chang et al., 2021) and it automatically produces files in a JSON format using the ICASA  
28 standards when possible ([https://github.com/Ottis1/fo\\_management\\_data\\_input](https://github.com/Ottis1/fo_management_data_input)). Examples of historical field activity events  
29 (e.g. planting and tillage) that are prepared through this application are being made available in the Field Observatory JSON  
30 files and visualized on the graphs (Fig. 5).

### 31 3.2 Online soil measurements

32 Since 2020, each ACA site was provided with four TEROs-12 soil sensors (METER Group, Inc. USA) (two sensors per field,  
33 control and treatment) measuring volumetric water content, electrical conductivity and temperature (Table 3). The automated  
34 sensors are located at 75 mm depth in two of the three fixed measurement points of each field. The sensors were connected to  
35 a third party data transfer hardware (Datasense Oy, Finland), which uses Lora/WAN network to transmit the data. During the  
36 first year, the sensors measured every half hour but in 2021 measurement frequency was changed to one hour. The data is  
37 stored at the service providers server and is pulled to the PEcAn server (#8) through the Datasense API. Currently the sensor  
38 array includes 80 TEROs-12 soil sensors, four O<sub>2</sub> sensors (Apogee Instruments, USA) and two CO<sub>2</sub> sensors (Vaisala Oy,  
39 Finland) and will be supplemented with weather and groundwater depth measurements.

### 40 3.3 Online eddy covariance tower measurements

41 Carbon dioxide, evapotranspiration (latent heat), sensible heat and momentum fluxes between the ecosystem and atmosphere  
42 are measured at the intensive study sites, Ruukki and Qvidja, using the micrometeorological eddy covariance (EC) technique.  
43 The EC instrumentation at both sites includes a three-axis sonic anemometer (uSonic-2 Scientific, METEK GmbH, Elmshorn,  
44 Germany) and an enclosed-path infrared gas analyser (LI-7200, LI-COR Biosciences, NE, USA) installed on a tower. The  
45 measurement height is 2.3 m in Qvidja and 3.3 m in Ruukki (2.3 m from 13 June to 25 June 2019 and 3.1 m from 25 June to  
46 4 November 2019). For details of the measurement set-up in Qvidja, see Heimsch et al. (2021).

47 The data from the EC instruments are recorded at a 10-Hz frequency. Half-hourly turbulent fluxes are calculated by block-  
48 averaging these raw data after applying a double rotation of the coordinate system (McMillen, 1988). The time lag between  
49 the sonic anemometer and gas analyzer signals is determined based on the cross-correlation analysis (Rebmann et al., 2012).  
50 The gas fluxes are calculated from the mixing ratios determined with respect to dry air (Webb et al., 1980). The measured  
51 fluxes are compensated for the losses due to high-frequency signal attenuation within the measurement system (Laurila et al.,  
52 2005). The flux data are filtered for instrument malfunction and unfavourable flow conditions according to the following





53 validity criteria: number of spikes in the raw data < 100, mean CO<sub>2</sub> mixing ratio > 350 ppm, relative stationarity (Foken and  
54 Wichura, 1996) < 30 % and CO<sub>2</sub> mixing ratio variance < 15 ppm<sup>2</sup> from April to September and < 5 ppm<sup>2</sup> from October to  
55 March. At the Ruukki site, flux data are accepted from the wind direction sector 135°-315° (Blocks 5, 6, 5up and 6up) and the  
56 sectors 0°-90° and 330°-360° (Blocks 1-4). In Qvidja, the wind directions representing the direction of the experimental site  
57 are 0°-30° and 140°-360°. Periods of weak turbulence are filtered by applying a friction velocity threshold. The threshold and  
58 its uncertainty are estimated for each site-year using the moving-point-transition method (Reichstein et al., 2005) and a  
59 bootstrapping approach (Pastorello et al., 2020). For incomplete years, the estimates from the previous year are used.

60 The EC measurements are complemented with supporting meteorological observations conducted next to the flux tower. These  
61 include soil moisture, soil temperature at different depths, soil heat flux, photosynthetically active radiation (PAR), global and  
62 reflected solar radiation, air temperature and precipitation. Half-hourly meteorological and flux data are transmitted to a server  
63 at the FMI, which is then synchronized to the PEcAn server (#8).

### 64 3.3.1 Flux data processing

65 The missing CO<sub>2</sub> flux (net ecosystem exchange, NEE) data are gap-filled based on empirical response functions that are fitted  
66 separately for the gross primary production (GPP) and total ecosystem respiration (ER):

$$67 \quad NEE = GPP + ER \quad (1)$$

68 Respiration is modelled as a function of air temperature:

$$69 \quad ER = R_0 \cdot e^{E_0 \left( \frac{1}{T_0} - \frac{1}{T_a - T_1} \right)} \quad (2)$$

70 where  $R_0$  is the respiration rate at the reference temperature of 283.15 K,  $T_0 = 227.13$  K,  $T_1 = 56.02$  K,  $E_0$  is the temperature  
71 sensitivity of respiration, and  $T_a$  is the measured air temperature (Lloyd and Taylor, 1994).

72 GPP is modelled as a function of PAR:

$$73 \quad GPP = \frac{\alpha \cdot PAR \cdot GP_{max}}{\alpha \cdot PAR + GP_{max}} \quad (3)$$

74 where  $\alpha$  is the apparent quantum yield and  $GP_{max}$  is the asymptotic photosynthesis rate in optimal light conditions.

75 For gap-filling, the data are divided into blocks based on the harvest dates, and each block is gap-filled separately. First,  $R_0$   
76 and  $E_0$  are estimated from the night-time ( $PAR < 20 \mu\text{mol m}^{-2} \text{s}^{-1}$ ) flux data with a 15-day moving window. If there are less  
77 than 25 observations, the window size is increased stepwise by two days until enough data are obtained. Similarly,  $\alpha$  and  $GP_{max}$   
78 are determined with a three-day moving window by fitting the PAR response function to the daytime NEE from which the



79 modelled respiration is subtracted. Gap-filled values that are determined using fits from asymmetrical time windows, with  
80 possibly biased data are flagged and updated when new measurements become available. Before flux gap-filling, the missing  
81 air temperature and PAR data are imputed using linear interpolation if the gap is not longer than 6 h. Longer gaps are filled  
82 using the mean diel cycle of the data measured within seven days before or after the missing data point

83 The uncertainty of measured NEE ( $E_{\text{meas}}$ ) is inferred from the model residuals. For each site-year, the measurements are  
84 grouped into  $0.2 \text{ mg CO}_2 \text{ m}^{-2} \text{ s}^{-1}$  wide bins, and for each bin the measurement uncertainty is characterized as the standard  
85 deviation of the residuals. The uncertainty of each measured half-hourly flux is then estimated from the relation between the  
86 measurement uncertainty and the magnitude of the flux (Richardson et al., 2008). For incomplete years, the relation from the  
87 previous year is used.

88 The uncertainty of modelled NEE ( $E_{\text{mod}}$ ) is propagated from the uncertainties of the least-squares fits of modelled GPP ( $E_{\text{GPP}}$ )  
89 and Reco ( $E_{\text{Reco}}$ ) as:

$$90 \quad E_{\text{mod}} = \sqrt{E_{\text{GPP}}^2 + E_{\text{Reco}}^2} \quad (4)$$

91 Finally, the uncertainty related to the friction velocity threshold ( $E_{\text{ustar}}$ ) is estimated by filtering the flux data using the 100  
92 different bootstrapped friction velocity thresholds, gap-filling the 100 differently filtered datasets, and using the standard  
93 deviation of the gap-filled fluxes as an estimate for  $E_{\text{ustar}}$ .

### 94 **3.4 FMI open weather data**

95 For all ACA sites, the weather information, namely precipitation, air temperature, relative humidity, wind speed and wind  
96 direction are retrieved from the nearest FMI weather stations (Table 2). Weather data are pulled to the PEcAn server using the  
97 fmir R package (<https://github.com/mikmart/fmir>).

### 98 **3.5 Satellite data from Google Earth Engine (GEE)**

99 All sites are monitored using remote sensing imagery from European Space Agency's (ESA) Sentinel-2 satellites.  
100 Atmospherically corrected Level-2A (L2A) Sentinel-2 multispectral data are retrieved using GEE ([earthengine.google.com](http://earthengine.google.com))  
101 cloud data platform. The scene classification band available in L2A products is used to filter away image acquisition dates  
102 during which the field is covered by snow, cloud or cloud shadow. Normalized Difference Vegetation Index (NDVI) is  
103 calculated using near infra-red (B8A) and red (B4) bands of the L2A products. The Leaf Area Index (LAI) is estimated using  
104 the ESA Sentinel Application Platform (SNAP) Biophysical Processor neural network algorithm (Weiss & Baret, 2016,  
105 <https://github.com/ollinevalainen/satellitertools>). The NDVI data is natively available in 10 m resolution, whereas LAI is  
106 resampled to 10 m resolution from its original 20 m resolution. The satellite data is updated every two days at most (which is  
107 the Sentinel-2 revisit frequency over Finland). In addition, yearly cumulative NDVI sum is calculated using integration by



08 trapezoidal rule for all sites (“NDVI days”). Common starting and ending points for the active growing season, 31 March and  
09 31 October, respectively, are used to standardize the cumulative NDVI sums between sites. To improve within site comparison,  
10 the cumulative NDVI is computed using dates when all fields within a site have satellite imagery available. The NDVI and  
11 LAI data is provided to the Field Observatory user interface in both raster (GeoTIFF) and tabular form (CSV).

12 With the tabular data, the average value of pixels within the field is used to estimate the field-level value. The tabular data is  
13 provided with 90 % confidence intervals by multiplying the associated uncertainties by 1.645. Non-realistic negative LAI  
14 values are capped to zero. For NDVI the uncertainty is presented as standard error of the mean (SE) of the pixels within the  
15 field. For the cumulative NDVI sum, the uncertainties are propagated using the Python uncertainties package  
16 (<https://pythonhosted.org/uncertainties/>) which automatically computes the required derivatives and propagates the  
17 uncertainties .

18 The uncertainty for the LAI ( $u_{LAI}$ ) is estimated by combining observational uncertainty ( $SE_{LAI}$ ) and the algorithmic  
19 uncertainty ( $u_{alg}$ ) of the LAI estimation:

$$20 \quad u_{LAI} = \sqrt{SE_{LAI}^2 + u_{alg}^2}, \quad (5)$$

21 where the  $SE_{LAI}$  is computed as the SE of LAI observations within the field. The  $u_{alg}$  is calculated by propagating individual  
22 pixel uncertainties ( $u_{t_i}$ ) to the calculated average:

$$23 \quad u_{alg} = n^{-1} \sqrt{\sum_{i=1}^n u_{t_i}^2}, \quad (6)$$

24 where n is the number of pixels (i.e. sample size) and  $u_t$  the reported theoretical RMSE for the SNAP LAI algorithm that is  
25 0.89 (Weiss and Baret, 2016) and constant to all pixels. The artificial increase of n due to resampling LAI observations from  
26 its native 20 m resolution to 10 m is taken into account and n is reduced accordingly.

### 27 **3.6 PAR from Copernicus Atmospheric Monitoring Service (CAMS)**

28 For the ACA sites, the daily PAR data are derived from the global irradiation data obtained from the CAMS through daily  
29 queries ([www.soda-pro.com/web-services/radiation/cams-radiation-service/](http://www.soda-pro.com/web-services/radiation/cams-radiation-service/), Qu et al., 2017). The global daily irradiation (Wh  
30  $\text{m}^{-2} \text{day}^{-1}$ ) is converted to daily PAR ( $\text{MJ m}^{-2} \text{day}^{-1}$ ) assuming that 50 % of the global irradiation is at PAR range. The CAMS  
31 data is available for each day with a 48 h time lag. The daily PAR is reported in  $\text{MJ m}^{-2} \text{day}^{-1}$  which is a more convenient unit  
32 for a daily value compared to  $\mu\text{mol m}^{-2} \text{s}^{-1}$  used with 30-min measurement frequency in intensive sites.



### 33 3.7 ECMWF 15-day ensemble weather forecasts

34 European Center Medium-range Weather Forecast (ECMWF) data are processed by the Finnish Meteorological Institute for  
 35 every site. This dataset consists of 6-hourly 2 meter temperature ( $2t$  variable in ECMWF standards), total precipitation ( $tp$ ),  
 36 relative humidity ( $r$ ), 10 meter U and V wind components ( $10u$  and  $10v$ , respectively), surface pressure ( $sp$ ), surface solar and  
 37 thermal radiation downwards ( $ssrd$  and  $strd$ , respectively) values of 51 ensemble members where one member is the control  
 38 forecast and the other 50 are perturbed members which have perturbed initial conditions different than the control to explore  
 39 the range of uncertainty (Buizza and Richardson, 2017). Weather forecast data are updated everyday. Per ECMWF license  
 40 agreements, the data are visualized as is but the disseminated tabular files are obfuscated.

41 **Table 3 Summary of data streams reported in FiON. Offline = stored in public data repository and updated as necessary.**

Data type	Units	Data source	Frequency	Since	Sites	Online/offline
Field activity	-	Personal communication*	Seasonal	2019	All	Offline
Farmer management actions	-	Questionnaire	Annual		All	Offline
Soil C	% (ACA), kg m <sup>-2</sup> (Qvidja)	Lab measurements	Biannual	2018	All, except Ruukki	Offline
Soil water holding capacity	m <sup>3</sup> m <sup>-3</sup>	Lab measurements	Once to calibrate sensors	2019	All, except Ruukki	Offline
Soil nutrients	mg kg <sup>-1</sup>	Lab measurements	Biannual	2018	ACA	Offline
Bulk density	kg dm <sup>-3</sup>	Lab measurements	Annual	2019	ACA	Offline
Biomass	kg ha <sup>-1</sup>	Lab measurements	Annual	2019	ACA	Offline
Soil moisture	m <sup>3</sup> m <sup>-3</sup>	ACA soil sensors & eddy covariance	Half-hourly	2018 (Qvidja), 2019 (Ruukki), 2020 (ACA)	ACA & Intensive	Online
Soil temperature	°C	ACA soil sensors & eddy covariance	Half-hourly	2018 (Qvidja), 2019 (Ruukki), 2020 (ACA)	ACA & Intensive	Online
Electrical conductivity	µS cm <sup>-1</sup>	ACA soil sensors	Half-hourly	2020	ACA	Online
CO <sub>2</sub> -flux	mg m <sup>-2</sup> s <sup>-1</sup>	Eddy covariance	Half-	2018 (Qvidja),	Intensive	Online



	<sup>1</sup>		hourly	2019 (Ruukki)	e	
Latent and sensible heat flux	W m <sup>-2</sup>	Eddy covariance	Half-hourly	2018 (Qvidja), 2019 (Ruukki)	Intensive	Online
Short-wave radiation (incoming and reflected)	W m <sup>-2</sup>	Eddy covariance	Half-hourly	2018 (Qvidja), 2019 (Ruukki)	Intensive	Online
CO <sub>2</sub> concentration	ppm	Eddy covariance	Half-hourly	2018 (Qvidja), 2019 (Ruukki)	Intensive	Online
Precipitation	mm	FMI open weather & eddy covariance	Half-hourly	2018 (Qvidja), 2019 (ACA & Ruukki)	ACA & Intensive	Online
Air Temperature	°C	FMI open weather & eddy covariance	Half-hourly	2018 (Qvidja), 2019 (ACA & Ruukki)	ACA & Intensive	Online
Relative Humidity	%	FMI open weather & eddy covariance	Half-hourly	2018 (Qvidja), 2019 (ACA & Ruukki)	ACA & Intensive	Online
PAR	MJ m <sup>-2</sup> day <sup>-1</sup> μmol m <sup>-2</sup> s <sup>-1</sup>	Copernicus & eddy covariance	Daily & half-hourly	2018 (Qvidja), 2019 (ACA & Ruukki)	ACA & Intensive	Online
Leaf Area Index	m <sup>2</sup> m <sup>-2</sup>	Sentinel-2, GEE	Min 2-days	2018 (Qvidja), 2019 (ACA & Ruukki)	All	Online
NDVI	-	Sentinel-2, GEE	Min 2-days	2018 (Qvidja), 2019 (ACA & Ruukki)	All	Online

42 \*Online application is under development.

### 43 3.8 Predictive Ecosystem Analyzer (PEcAn) server

44 All FiON data are pooled in an FMI server where model-data integration cyberinfrastructure software PEcAn is installed and  
 45 compiled. PEcAn is an ecological informatics toolbox that consists of process-based models, a workflow management system  
 46 and analytical tools for model-data synthesis (LeBauer et al., 2013; Dietze et al., 2013). The automated PEcAn workflow calls  
 47 a series of modularized tasks that involve pre-processing of the model inputs, configuring and running the models, post-  
 48 processing model outputs and performing model-data integration analyses. Coupling a process-based model to this workflow



49 requires writing a model package which consists of a few interfacing scripts as PEcAn adopts intermediate input and output  
50 file formats, and applies pre- and post-model run analyses to these standards (Fer et al., 2021). While there are already many  
51 ecosystem models coupled to PEcAn and its design is general across process-based models, coupling of more models that can  
52 simulate agricultural ecosystems is in progress. In this study, we coupled the BASGRA\_N model (Basic Grassland Model,  
53 Höglind et al., 2020) to the PEcAn workflow and demonstrated its use for the Qvidja site (see Sect. 4, Model-data synthesis).  
54 In the future, we will provide model predictions for all sites through PEcAn.

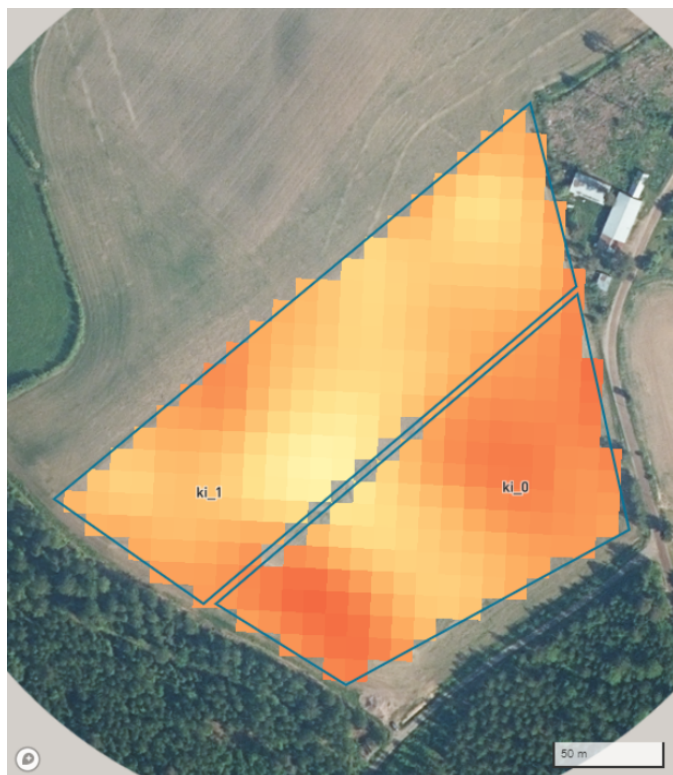
### 55 **3.9 Public data storage**

56 To harmonize the data, all tabular data with less than daily measurement frequency is aggregated to a 30 min interval (to every  
57 hour and half hour) before transferring the data to the public data storage (Amazon Simple Storage Service, field-  
58 observatory.data.lit.fmi.fi). To protect the privacy of the farmers, all data holding spatial information is transformed for all  
59 ACA sites, except for site MU (which is operated by Häme University of Applied Sciences).

### 60 **3.10 Field Observatory user interface**

61 The Field Observatory user interface (v1.0, fieldobservatory.org) allows viewing general information about the sites and the  
62 measurements and carbon farming practices conducted on them. The website has an interactive map to navigate to site-specific  
63 dashboards. A site view consists of general information about the site, an interactive map with satellite imagery of a specified  
64 vegetation parameter, an interactive timeline for selecting satellite imagery for viewing, and a panel of interactive time series  
65 charts (Fig. 3). Each chart comes with a description of the displayed data. A chart typically contains multiple time series and  
66 the visibility of each can be toggled. The user can enable and disable time aggregation and choose the time aggregation level  
67 from predefined options. The time aggregation is calculated using sliding statistics such as mean or sum depending on the data  
68 type. Any chart can be exported as an SVG image or as a CSV file containing the displayed data. A global specification file  
69 defines a list of charts and the data source types that can be shown in each chart. Site-specific specification files are used to  
70 define data source types available for each site and to provide links to the data files. Specification files are stored in JSON  
71 format.

72 The website is served by Azure services. The map and site views are based on client-side JavaScript, running in the user's web  
73 browser. Maps have been implemented using Mapbox GL JS JavaScript library.



74

75

76

77

(a)

## KI

Advanced CarbonAction Site

KI field is a low OM sand in organic crop rotation. The aim is to increase OM by adding organic matter through soil amendments (wood pulp, ramial woodchips).

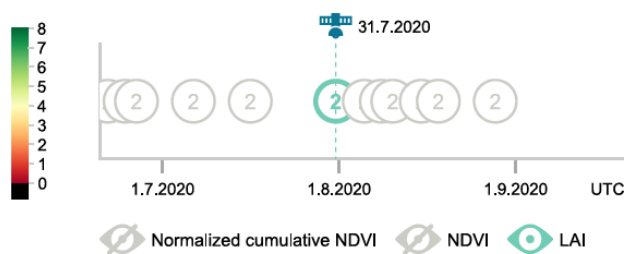
### FARMING METHODS

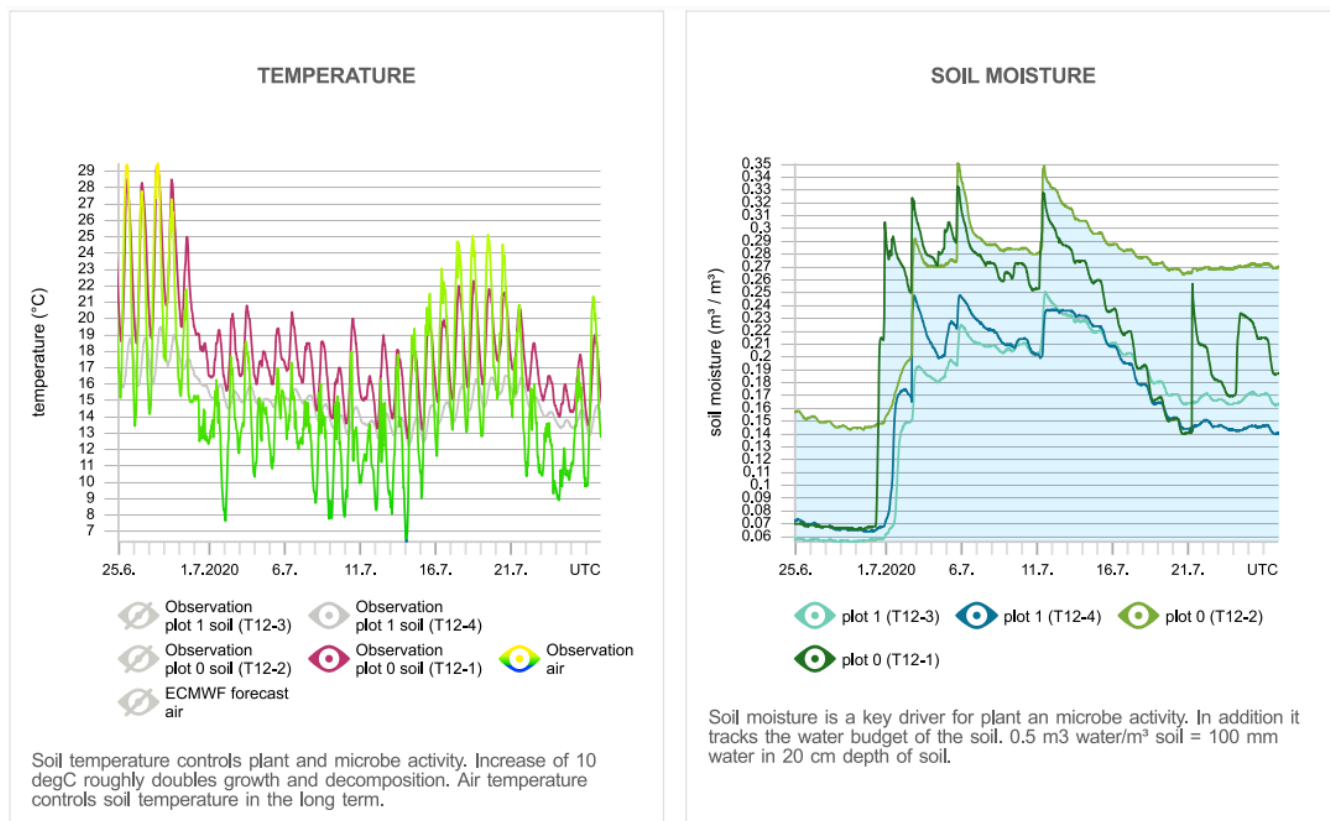
Management: soil amendments

Species: multi-species ley

Soil type: fine sand

### SATELLITE IMAGES





78

79

(b)

80 **Figure 3** Two web interface views of the measurement data for site KI: (a) Overview and LAI satellite images and (b) observed  
81 soil and air temperature and soil moisture. The reader is referred to the website [www.fieldobservatory.org](http://www.fieldobservatory.org) for more and  
82 interactive charts. The aerial photo contains data from the National Land Survey of Finland Topographic Database (11/2020).

#### 83 **4 Model-data synthesis and decision support**

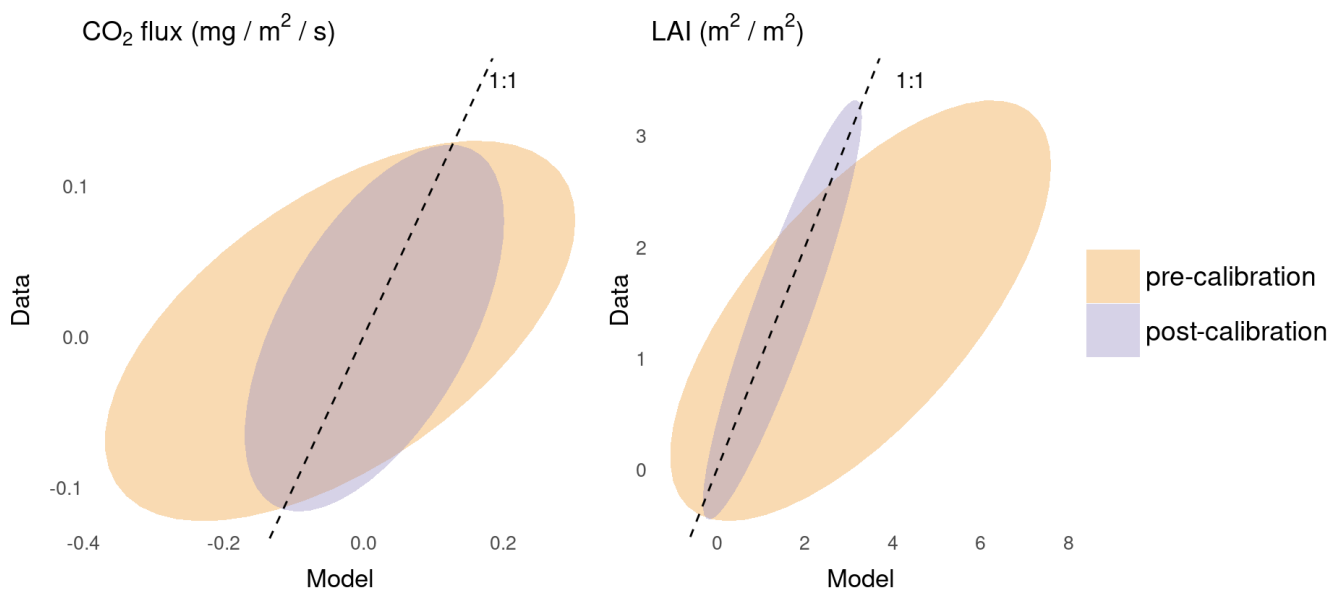
84 While the current version of the Field Observatory mainly disseminates observations, one of the main goals of this application  
85 is to provide accessible near real-time model-data synthesis, forecasting and decision support for the users. We demonstrate  
86 the first application of this service at the Qvidja grassland site with the grassland model BASGRA\_N (Table 2). BASGRA\_N  
87 model is developed specifically for northern climates and for grass types (timothy, *Phleum pratense*; meadow fescue, *Festuca  
88 pratensis*) that are the dominating forage species cultivated at the Qvidja farm, and it is able to simulate grassland productivity,  
89 quality and greenhouse gas balance (Höglind et al., 2020).

90





91 We coupled BASGRA\_N to PEcAn, and used PEcAn's workflow management system and analytical tools (specifically the  
92 Bayesian calibration and state data assimilation modules) to inform the model with the data. Before employing them for  
93 forecasting and decision support, these models need to be initialized and calibrated. Therefore, we used the field and lab  
94 measurements (Sect. 3.1), such as the rooting depth, soil carbon content and soil water holding capacity, to initialize the model  
95 states. Next, using multiple constraints (CO<sub>2</sub> flux and LAI from the eddy covariance tower field, Sect. 3.3), we calibrated 20  
96 model parameters using Bayesian numerical methods through the BayesianTools R-package (Hartig et al., 2019) as  
97 implemented in the PEcAn system (Fer et al., 2018). In calibration, we used the observations from May 2018 to April 2021.  
98 After calibration model predictions were improved in terms of both uncertainty reduction and accuracy (Fig. 4).



99  
00

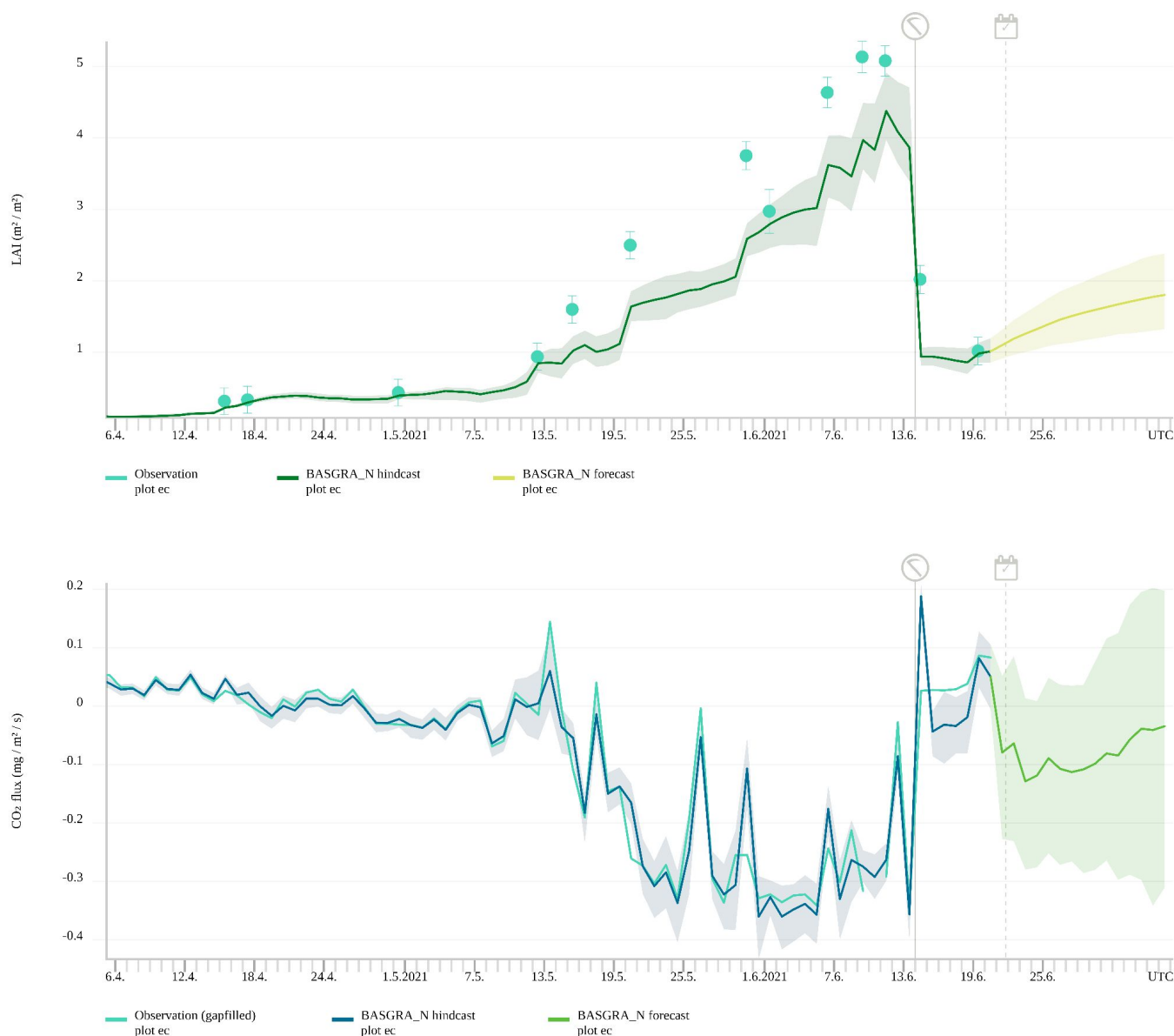
01 **Figure 4** Predicted versus observed comparison before (orange ellipses) and after (purple ellipses) initialization and  
02 calibration. Ellipses represent the 90% CI of model ensemble runs with 500 members. After initialization and calibration, the  
03 model performance at Qvidja improved in terms of both accuracy (closer to the 1:1 line) and uncertainty reduction (narrower  
04 ellipses).

05

06 Next, we deployed the initialized and calibrated model in an online, operational, iterative near-term forecasting framework by  
07 driving it with the ECMWF ensemble 15-day weather forecast (Sect. 3.7). From April 2021 onwards, every day a 15-day  
08 ensemble forecast is made from the BASGRA\_N model. As time progresses, each day the CO<sub>2</sub> flux forecast is informed with  
09 the observed and gap-filled daily CO<sub>2</sub> flux values within an iterative forecast-analysis cycle using the Extended Ensemble  
10 Kalman filter algorithm implemented in PEcAn (Dietze, 2017). When LAI observations are also available, they are jointly  
11 assimilated with the CO<sub>2</sub> flux measurements as well. Although we are currently only assimilating the CO<sub>2</sub> flux and LAI  
12 observations, related states are also updated within the model through the analysis step as the model encodes and simulates



13 relations and covariances among different ecosystem processes. Among the model output variables, we share the LAI and CO<sub>2</sub>  
14 flux (Fig. 5), as well as Latent Heat and Yield Potential forecasts with the users through the Field Observatory user interface,  
15 albeit only for the Qvidja site for the time being.



16  
17 **Figure 5** 15-day LAI (top) and CO<sub>2</sub> flux (bottom) forecast at Qvidja. The 90 % confidence intervals for hindcast and forecast  
18 are generated by 250 ensemble members, with different combinations of model parameters, initial conditions and  
19 meteorological drivers. Units in the CO<sub>2</sub> flux graph are given per second to reflect the measurement frequency, however,



20 observations were aggregated to daily time step here to align with the model predictions. The scythe icon indicates a harvest  
21 event on June 14th, 2021.

## 22 **5 Discussion**

23 This paper introduced the Field Observatory Network (FiON) and its unified methodology leading the way to monitor and  
24 forecast the functioning of agricultural ecosystems, geared towards verification of soil carbon sequestration. This methodology  
25 combines the existing spatially scattered measurements, modeling and computing networks, and disseminates the model-data  
26 computation outcomes through the Field Observatory user interface. In the following, we discuss the scientific and practical  
27 contributions of FiON and the Field Observatory, and the future steps planned for both.

### 28 **5.1 Scientific contribution**

29 FiON adopts state-of-the-art field and laboratory methods, open data sources, near real-time satellite imagery processing and  
30 model-data integration cyberinfrastructures—all of which are needed for a reliable MRV platform. A distinct feature of FiON  
31 is the network of ordinary farms, ACA sites, to establish baseline trends and verify additional changes. As soil carbon pool  
32 changes slowly, even after a shift in management practices, long-term monitoring is needed. The ACA sites (with control and  
33 treatment plots) were specifically designed for this purpose and will be monitored continuously for at least the next five years,  
34 and FiON aspires to continue even longer. This is an adequate time frame to detect SOC changes because the fastest carbon  
35 re-accumulation occurs in the first 10–20 years, depending on soil type, management practices, climate and initial SOC (Bossio  
36 et al., 2020), all of which are monitored by FiON. The intensive and ACA sites provide an important benchmarking opportunity  
37 to our model-data synthesis methodology which will be applied to all 100 Carbon Action farms. The PEcAn platform is central  
38 to our methodology; it enables synthesizing different data sources and process-based models, managing observational and  
39 model uncertainties, and near real-time forecasting. It distinguishes FiON from observations-only approaches.

### 40 **5.2 Practical contribution**

41 The Field Observatory user interface has not only enabled farmers to monitor impacts of their carbon farming practices, but  
42 also to connect and compare their own and others' data and practices. Features in the user interface are co-created with the  
43 farmers and developed accordingly. For example, farmers requested to see a cumulative sum of NDVI through the growing  
44 season which was in return calculated and included on the website. Likewise, simple and clear descriptions to interpret each  
45 data type have been found helpful. The gap-filled CO<sub>2</sub> fluxes at the intensive study sites have made it easier to communicate  
46 carbon exchanges between land and the atmosphere and how carbon budget calculations are done. As a result, the Field  
47 Observatory has already been used in workshops and meetings with stakeholders, and in training and scientific outreach for  
48 the Carbon Action farmers.



49  
50 One of our aims with this framework is to provide decision support for the end users. Although such functionality is not fully  
51 in place yet (but planned for the future versions), establishing the operational data assimilation and iterative forecasting pipeline  
52 is a milestone towards this direction. Users are quantitatively informed about the progression of various ecosystem states and  
53 services by these Field Observatory near-term forecast updates. The current pipeline is further being developed to improve the  
54 model performance and to be put into an adaptive decision making framework where alternative scenarios will be simulated  
55 with the model to aid users in their day-to-day operations.

56  
57 There is a large interest towards adopting and developing Field Observatory further. Therefore, the website is under constant  
58 development with new features, and new information about carbon farming and findings of FiON are increasingly being made  
59 available.

### 60 61 **5.3 Avenues for future research and development**

62  
63 We have planned future steps for both FiON and the Field Observatory. The first step is to add more agricultural models to  
64 PEcAn. This enables us to extend model-data analysis to all FiON sites where different species and management practices are  
65 involved (i.e. other than grass harvest timing and amount). Coupling of one such additional model (Simulateur  
66 multIdisciplinaire pour les Cultures Standard, STICS, Brisson et al., 1998) to PEcAn has already been completed, and others  
67 are in progress. In the meantime, more sites will be added to FiON, not only in number but also in type. For example, with  
68 carbon-smart planning, urban vegetation also has potential to store more carbon. We study this also in FiON and consequently  
69 urban sites will be added. Another goal is to include forests and peatlands in FiON, which requires incorporating new process-  
70 based models in the FiON workflow. During the coming years, more field and laboratory measurement data will be collected  
71 and used to validate the model estimates and re-calibrate the models.

72  
73 The development of the online application to gather field activity data from farmers is also in progress. This application will  
74 not only allow using field activity data in visualization and model-data synthesis but it will also enable the farmers to simulate  
75 a predefined number of scenarios regarding their day-to-day operations by triggering automated PEcAn workflows—for  
76 example, given the next 15-day forecast they will be able to optimize the timing and amounts of their field activity. In this  
77 context, Field Observatory's interoperability with commercial farm management information systems needs to be studied.

78  
79 We are currently also investigating the use of satellite data sources other than Sentinel-2 in retrieving information on vegetation  
80 and soil properties. In addition to satellite imagery, drones could be used as a source of remote sensing data. Finally, the data  
81 streams used in data assimilation (to inform and update forecasts) will be increased and improvement in forecasting skills will  
82 be analyzed.



## 83 **6 Conclusions**

84 The Field Observatory Network (FiON) introduced in this paper is primarily a network of researchers, farmers, companies and  
85 other stakeholders developing carbon farming practices. FiON provides a unified methodology to monitor and forecast  
86 agricultural carbon sequestration by combining offline and near real-time field measurements, weather data, satellite imagery,  
87 modeling and computing networks. FiON disseminates data through the Field Observatory user interface  
88 ([www.fieldobservatory.org](http://www.fieldobservatory.org)). For farmers, FiON serves as a monitoring and decision support tool. In contrast to the mainstream  
89 decision support tools, FiON also provides the farmers access to other carbon farmers' data in the network. This enables  
90 comparisons and knowledge transfer between the carbon farmers.

91 FiON has several analogies to other ecological observatory networks, but unlike these existing networks, FiON is designed to  
92 provide near real-time information and forecasts concerning the carbon farming practices and to facilitate monitoring and  
93 verification of carbon sequestration. In this sense, FiON takes several steps forward from the mainstream of the ecological  
94 observatory networks known so far.

## 95 **7 Data availability**

96 The data displayed in the Field Observatory are available from the Field Observatory website ([www.fieldobservatory.org](http://www.fieldobservatory.org)) and  
97 from Amazon Simple Storage Service at <https://field-observatory.data.lit.fmi.fi/index.html>. Field measurements conducted at  
98 ACA sites in 2019 and 2020 are available from Zenodo data repository (Mattila, 2020; Mattila and Heinonen, 2021).

## 99 **8 Code availability**

00 The satellite data processing codes are available from a public GitHub repository  
01 (<https://github.com/ollinevalainen/satellitertools>). All PEcAn code is available openly on a GitHub repository  
02 (<https://github.com/PecanProject/pecan>). Field Activity data collection and curation application code which is under  
03 development is also available via GitHub ([https://github.com/Ottis1/fo\\_management\\_data\\_input](https://github.com/Ottis1/fo_management_data_input)). Rest of the codes by the  
04 authors are not yet openly available.  
05

## 06 **9 Author contribution**

07 Conceptualization, ON, ONi, IF, AJ, TM, OK, JK, LH, LM, PJ, LK, ÅS, AL, JHe, IK, JL; Data curation, ON, IF, ONi, TM,  
08 OKu; Formal Analysis, ON, IF, ONi, TM, LHe, HV, SG, TV, JV, JT, Funding acquisition, TM, LK, AL, TL, JHe, TA, IK, JL;  
09 Investigation, ON, IF, ONi, TM, LHe, HV, SG, TV, JV, JT; Methodology, ON, IF, ONi, TM, HV, LK, OKu, TV, JV, JT, JHe,



10 TA, JL; Project administration, TM, JK, LH, LK, ÅS, AL, TL, JHe, TA, IK, JL; Software, ON, ONi, IF, AJ, OK, OKu, HV,  
11 TV, JV, JT; Visualization, ON, ONi, IF, AJ, LM, PJ, OKu and comments from all; Writing – original draft preparation, all  
12 authors; Writing – review & editing, all authors.

## 13 **10 Competing interests**

14 The authors declare that they have no conflict of interest.

## 15 **11 Acknowledgments**

16 The work of HAMK has been conducted within the research project: *Carbon 4.0 - Analysis and utilization of biological data*  
17 *in complex carbon ecosystems* funded by the Ministry of Education and Culture (Finland). The work by FMI was supported  
18 by Business Finland [grant 6905/31/2018], The Strategic Research Council at the Academy of Finland [decision no 327214],  
19 the Academy of Finland Flagship Program [decision no 337552], the Ministry of Agriculture and Forestry of Finland [grant  
20 VN/5094/2021] and Maj and Tor Nessling foundation (grant 202000391). The work by SYKE was supported by The Strategic  
21 Research Council at the Academy of Finland [decision no 327350].

22  
23 The authors want to thank the 20 farmers who allowed testing the framework on their Carbon Action fields. We also thank the  
24 owner of Ruukki farm, Natural Resources Institute Finland (Luke), and their employees for making it possible to have a  
25 measurement site there. In addition, we are thankful for the owners and staff of Qvidja farm.

## 26 **References**

- 27 Bellamy, P. H., Loveland, P. J., Bradley, R. I., Lark, R. M., and Kirk, G. J. D.: Carbon losses from all soils across England  
28 and Wales 1978–2003, *Nature*, 437, 245–248, <https://doi.org/10.1038/nature04038>, 2005.
- 29 Bossio, D. A., Cook-Patton, S. C., Ellis, P. W., Fargione, J., Sanderman, J., Smith, P., Wood, S., Zomer, R. J., von Unger, M.,  
30 Emmer, I. M., and Griscom, B. W.: The role of soil carbon in natural climate solutions, *Nat Sustain*, 3, 391–398,  
31 <https://doi.org/10.1038/s41893-020-0491-z>, 2020.
- 32 Buizza, R. and Richardson, D.: 25 years of ensemble forecasting at ECMWF, <https://doi.org/10.21957/BV418O>, 2017.
- 33 Chang, W., Cheng, J., Allaire, J., Xie, Y., and McPherson, J.: Shiny: web application framework for R, 1, 2017, 2017.
- 34 Crowther, T. W., van den Hoogen, J., Wan, J., Mayes, M. A., Keiser, A. D., Mo, L., Averill, C., and Maynard, D. S.: The  
35 global soil community and its influence on biogeochemistry, *Science*, 365, eaav0550, <https://doi.org/10.1126/science.aav0550>,  
36 2019.



- 37 Dietze, M.: Ecological Forecasting, Princeton University Press, <https://doi.org/10.1515/9781400885459>, 2017.
- 38 Elmendorf, S. C., Jones, K. D., Cook, B. I., Diez, J. M., Enquist, C. A. F., Hufft, R. A., Jones, M. O., Mazer, S. J., Miller-  
39 Rushing, A. J., Moore, D. J. P., Schwartz, M. D., and Weltzin, J. F.: The plant phenology monitoring design for The National  
40 Ecological Observatory Network, *Ecosphere*, 7, e01303, <https://doi.org/10.1002/ecs2.1303>, 2016.
- 41 Fer, I., Kelly, R., Moorcroft, P. R., Richardson, A. D., Cowdery, E. M., and Dietze, M. C.: Linking big models to big data:  
42 efficient ecosystem model calibration through Bayesian model emulation, *Biogeosciences*, 15, 5801–5830,  
43 <https://doi.org/10.5194/bg-15-5801-2018>, 2018.
- 44 Fer, I., Gardella, A. K., Shiklomanov, A. N., Campbell, E. E., Cowdery, E. M., De Kauwe, M. G., Desai, A., Duveneck, M. J.,  
45 Fisher, J. B., Haynes, K. D., Hoffman, F. M., Johnston, M. R., Kooper, R., LeBauer, D. S., Mantooh, J., Parton, W. J., Poulter,  
46 B., Quaipe, T., Raiho, A., Schaefer, K., Serbin, S. P., Simkins, J., Wilcox, K. R., Viskari, T., and Dietze, M. C.: Beyond  
47 ecosystem modeling: A roadmap to community cyberinfrastructure for ecological data-model integration, *Glob. Change Biol.*,  
48 27, 13–26, <https://doi.org/10.1111/gcb.15409>, 2021.
- 49 Foken, Th. and Wichura, B.: Tools for quality assessment of surface-based flux measurements, *Agricultural and Forest  
50 Meteorology*, 78, 83–105, [https://doi.org/10.1016/0168-1923\(95\)02248-1](https://doi.org/10.1016/0168-1923(95)02248-1), 1996.
- 51 Guerra, C. A., Bardgett, R. D., Caon, L., Crowther, T. W., Delgado-Baquerizo, M., Montanarella, L., Navarro, L. M., Orgiazzi,  
52 A., Singh, B. K., Tedersoo, L., Vargas-Rojas, R., Briones, M. J. I., Buscot, F., Cameron, E. K., Cesarz, S., Chatzinotas, A.,  
53 Cowan, D. A., Djukic, I., van den Hoogen, J., Lehmann, A., Maestre, F. T., Marín, C., Reitz, T., Rillig, M. C., Smith, L. C.,  
54 de Vries, F. T., Weigelt, A., Wall, D. H., and Eisenhauer, N.: Tracking, targeting, and conserving soil biodiversity, *Science*,  
55 371, 239–241, <https://doi.org/10.1126/science.abd7926>, 2021.
- 56 Heikkinen, J., Ketoja, E., Nuutinen, V., and Regina, K.: Declining trend of carbon in Finnish cropland soils in 1974–2009,  
57 *Glob Change Biol*, 19, 1456–1469, <https://doi.org/10.1111/gcb.12137>, 2013.
- 58 Heikkinen, J., Keskinen, R., Regina, K., Honkanen, H., and Nuutinen, V.: Estimation of carbon stocks in boreal cropland soils  
59 - methodological considerations, *Eur J Soil Sci*, 72, 934–945, <https://doi.org/10.1111/ejss.13033>, 2021.
- 60 Heimsch, L., Lohila, A., Tuovinen, J.-P., Vekuri, H., Heinonsalo, J., Nevalainen, O., Korkiakoski, M., Liski, J., Laurila, T.,  
61 and Kulmala, L.: Carbon dioxide fluxes and carbon balance of an agricultural grassland in southern Finland, *Biogeosciences*,  
62 18, 3467–3483, <https://doi.org/10.5194/bg-18-3467-2021>, 2021.
- 63 Hinckley, E. S., Bonan, G. B., Bowen, G. J., Colman, B. P., Duffy, P. A., Goodale, C. L., Houlton, B. Z., Marín-Spiotta, E.,  
64 Ogle, K., Ollinger, S. V., Paul, E. A., Vitousek, P. M., Weathers, K. C., and Williams, D. G.: The soil and plant biogeochemistry  
65 sampling design for The National Ecological Observatory Network, *Ecosphere*, 7, <https://doi.org/10.1002/ecs2.1234>, 2016.



- 66 Hipsey, M. R., Bruce, L. C., Boon, C., Busch, B., Carey, C. C., Hamilton, D. P., Hanson, P. C., Read, J. S., de Sousa, E.,  
67 Weber, M., and Winslow, L. A.: A General Lake Model (GLM 3.0) for linking with high-frequency sensor data from the  
68 Global Lake Ecological Observatory Network (GLEON), *Geosci. Model Dev.*, 12, 473–523, [https://doi.org/10.5194/gmd-12-](https://doi.org/10.5194/gmd-12-473-2019)  
69 [473-2019](https://doi.org/10.5194/gmd-12-473-2019), 2019.
- 70 Höglind, M., Cameron, D., Persson, T., Huang, X., and van Oijen, M.: BASGRA\_N: A model for grassland productivity,  
71 quality and greenhouse gas balance, *Ecological Modelling*, 417, 108925, <https://doi.org/10.1016/j.ecolmodel.2019.108925>,  
72 2020.
- 73 Keller, M., Schimel, D. S., Hargrove, W. W., and Hoffman, F. M.: A continental strategy for the National Ecological  
74 Observatory Network, *Frontiers in Ecology and the Environment*, 6, 282–284, [https://doi.org/10.1890/1540-](https://doi.org/10.1890/1540-9295(2008)6[282:ACSFTN]2.0.CO;2)  
75 [9295\(2008\)6\[282:ACSFTN\]2.0.CO;2](https://doi.org/10.1890/1540-9295(2008)6[282:ACSFTN]2.0.CO;2), 2008.
- 76 Köchy, M., Hiederer, R., and Freibauer, A.: Global distribution of soil organic carbon – Part 1: Masses and frequency  
77 distributions of SOC stocks for the tropics, permafrost regions, wetlands, and the world, *SOIL*, 1, 351–365,  
78 <https://doi.org/10.5194/soil-1-351-2015>, 2015.
- 79 Lal, R., Negassa, W., and Lorenz, K.: Carbon sequestration in soil, *Current Opinion in Environmental Sustainability*, 15, 79–  
80 86, <https://doi.org/10.1016/j.cosust.2015.09.002>, 2015.
- 81 Laurila, T., Tuovinen, J.-P., Lohila, A., Hatakka, J., Aurela, M., Thum, T., Pihlatie, M., Rinne, J., and Vesala, T.: Measuring  
82 methane emissions from a landfill using a cost-effective micrometeorological method: MEASURING METHANE  
83 EMISSIONS, *Geophys. Res. Lett.*, 32, n/a-n/a, <https://doi.org/10.1029/2005GL023462>, 2005.
- 84 Lloyd, J. and Taylor, J. A.: On the Temperature Dependence of Soil Respiration, *Functional Ecology*, 8, 315,  
85 <https://doi.org/10.2307/2389824>, 1994.
- 86 Mattila, T.: Carbon action MULTA Finnish carbon sequestration experimental field dataset 2019,  
87 <https://doi.org/10.5281/ZENODO.3670654>, 2020.
- 88 Mattila, T., Hagelberg, E., Söderlund, S., and Joona, J.: How farmers approach carbon sequestration? Lessons learned from  
89 105 Carbon Farming Plans., Paper submitted to *Soil and Tillage Research*, 2021.
- 90 Mattila, Tuomas and Heinonen, Reija: Carbon action MULTA Finnish carbon sequestration experimental field dataset 2020,  
91 <https://doi.org/10.5281/ZENODO.4068271>, 2021.
- 92 McMillen, R. T.: An eddy correlation technique with extended applicability to non-simple terrain, *Boundary-Layer Meteorol.*,  
93 43, 231–245, <https://doi.org/10.1007/BF00128405>, 1988.





- 94 Meersmans, J., Van Wesemael, B., De Ridder, F., Fallas Dotti, M., De Baets, S., and Van Molle, M.: Changes in organic  
95 carbon distribution with depth in agricultural soils in northern Belgium, 1960–2006: CHANGES IN SOC OF NORTHERN  
96 BELGIUM, 15, 2739–2750, <https://doi.org/10.1111/j.1365-2486.2009.01855.x>, 2009.
- 97 Merante, P., Dibari, C., Ferrise, R., Sánchez, B., Iglesias, A., Lesschen, J. P., Kuikman, P., Yeluripati, J., Smith, P., and Bindi,  
98 M.: Adopting soil organic carbon management practices in soils of varying quality: Implications and perspectives in Europe,  
99 Soil and Tillage Research, 165, 95–106, <https://doi.org/10.1016/j.still.2016.08.001>, 2017.
- 00 Minasny, B., Malone, B. P., McBratney, A. B., Angers, D. A., Arrouays, D., Chambers, A., Chaplot, V., Chen, Z.-S., Cheng,  
01 K., Das, B. S., Field, D. J., Gimona, A., Hedley, C. B., Hong, S. Y., Mandal, B., Marchant, B. P., Martin, M., McConkey, B.  
02 G., Mulder, V. L., O'Rourke, S., Richer-de-Forges, A. C., Odeh, I., Padarian, J., Paustian, K., Pan, G., Poggio, L., Savin, I.,  
03 Stolbovoy, V., Stockmann, U., Sulaeman, Y., Tsui, C.-C., Vågen, T.-G., van Wesemael, B., and Winowiecki, L.: Soil carbon  
04 4 per mille, Geoderma, 292, 59–86, <https://doi.org/10.1016/j.geoderma.2017.01.002>, 2017.
- 05 Oldfield, E. E., Wood, S. A., and Bradford, M. A.: Direct effects of soil organic matter on productivity mirror those observed  
06 with organic amendments, Plant Soil, 423, 363–373, <https://doi.org/10.1007/s11104-017-3513-5>, 2018.
- 07 Pastorello, G., Trotta, C., Canfora, E., Chu, H., Christianson, D., Cheah, Y.-W., Poindexter, C., Chen, J., Elbashandy, A.,  
08 Humphrey, M., Isaac, P., Polidori, D., Reichstein, M., Ribeca, A., van Ingen, C., Vuichard, N., Zhang, L., Amiro, B., Ammann,  
09 C., Arain, M. A., Ardö, J., Arkebauer, T., Arndt, S. K., Arriga, N., Aubinet, M., Aurela, M., Baldocchi, D., Barr, A.,  
10 Beamesderfer, E., Marchesini, L. B., Bergeron, O., Beringer, J., Bernhofer, C., Berveiller, D., Billesbach, D., Black, T. A.,  
11 Blanken, P. D., Bohrer, G., Boike, J., Bolstad, P. V., Bonal, D., Bonnefond, J.-M., Bowling, D. R., Bracho, R., Brodeur, J.,  
12 Brümmer, C., Buchmann, N., Burban, B., Burns, S. P., Buysse, P., Cale, P., Cavagna, M., Cellier, P., Chen, S., Chini, I.,  
13 Christensen, T. R., Cleverly, J., Collalti, A., Consalvo, C., Cook, B. D., Cook, D., Coursolle, C., Cremonese, E., Curtis, P. S.,  
14 D'Andrea, E., da Rocha, H., Dai, X., Davis, K. J., Cinti, B. D., Grandcourt, A. de Ligne, A. D., De Oliveira, R. C., Delpierre,  
15 N., Desai, A. R., Di Bella, C. M., Tommasi, P. di, Dolman, H., Domingo, F., Dong, G., Dore, S., Duce, P., Dufrêne, E., Dunn,  
16 A., Dušek, J., Eamus, D., Eichelmann, U., ElKhidir, H. A. M., Eugster, W., Ewenz, C. M., Ewers, B., Famulari, D., Fares, S.,  
17 Feigenwinter, I., Feitz, A., Fensholt, R., Filippa, G., Fischer, M., Frank, J., Galvagno, M., et al.: The FLUXNET2015 dataset  
18 and the ONEFlux processing pipeline for eddy covariance data, Scientific Data, 7, 225, [https://doi.org/10.1038/s41597-020-](https://doi.org/10.1038/s41597-020-0534-3)  
19 [0534-3](https://doi.org/10.1038/s41597-020-0534-3), 2020.
- 20 Qu, Z., Oumbe, A., Blanc, P., Espinar, B., Gesell, G., Gschwind, B., Klüser, L., Lefèvre, M., Saboret, L., Schroedter-  
21 Homscheidt, M., and Wald, L.: Fast radiative transfer parameterisation for assessing the surface solar irradiance: The  
22 Heliosat-4 method, Meteorol Z, 26, 33–57, <https://doi.org/10.1127/metz/2016/0781>, 2017.
- 23 Rebmann, C., Kolle, O., Heinesch, B., Queck, R., Ibrom, A., and Aubinet, M.: Data Acquisition and Flux Calculations, in:  
24 Eddy Covariance, edited by: Aubinet, M., Vesala, T., and Papale, D., Springer Netherlands, Dordrecht, 59–83,  
25 [https://doi.org/10.1007/978-94-007-2351-1\\_3](https://doi.org/10.1007/978-94-007-2351-1_3), 2012.



- 26 Reichstein, M., Falge, E., Baldocchi, D., Papale, D., Aubinet, M., Berbigier, P., Bernhofer, C., Buchmann, N., Gilmanov, T.,  
27 Granier, A., Grunwald, T., Havrankova, K., Ilvesniemi, H., Janous, D., Knohl, A., Laurila, T., Lohila, A., Loustau, D.,  
28 Matteucci, G., Meyers, T., Miglietta, F., Ourcival, J.-M., Pumpanen, J., Rambal, S., Rotenberg, E., Sanz, M., Tenhunen, J.,  
29 Seufert, G., Vaccari, F., Vesala, T., Yakir, D., and Valentini, R.: On the separation of net ecosystem exchange into assimilation  
30 and ecosystem respiration: review and improved algorithm, *Global Change Biol*, 11, 1424–1439,  
31 <https://doi.org/10.1111/j.1365-2486.2005.001002.x>, 2005.
- 32 Richardson, A. D., Mahecha, M. D., Falge, E., Kattge, J., Moffat, A. M., Papale, D., Reichstein, M., Stauch, V. J., Braswell,  
33 B. H., Churkina, G., Kruijt, B., and Hollinger, D. Y.: Statistical properties of random CO<sub>2</sub> flux measurement uncertainty  
34 inferred from model residuals, *Agricultural and Forest Meteorology*, 148, 38–50,  
35 <https://doi.org/10.1016/j.agrformet.2007.09.001>, 2008.
- 36 Saby, N. P. A., Arrouays, D., Antoni, V., Lemerrier, B., Follain, S., Walter, C., and Schwartz, C.: Changes in soil organic  
37 carbon in a mountainous French region, 1990–2004, 24, 254–262, <https://doi.org/10.1111/j.1475-2743.2008.00159.x>, 2008.
- 38 Sanderman, J., Hengl, T., and Fiske, G. J.: Soil carbon debt of 12,000 years of human land use, *Proc Natl Acad Sci USA*, 114,  
39 9575–9580, <https://doi.org/10.1073/pnas.1706103114>, 2017.
- 40 Smith, P., Soussana, J., Angers, D., Schipper, L., Chenu, C., Rasse, D. P., Batjes, N. H., Egmond, F., McNeill, S., Kuhnert,  
41 M., Arias-Navarro, C., Olesen, J. E., Chirinda, N., Fornara, D., Wollenberg, E., Álvaro-Fuentes, J., Sanz-Cobena, A., and  
42 Klumpp, K.: How to measure, report and verify soil carbon change to realize the potential of soil carbon sequestration for  
43 atmospheric greenhouse gas removal, *Glob Change Biol*, 26, 219–241, <https://doi.org/10.1111/gcb.14815>, 2020.
- 44 VandenBygaart, A. J. and Angers, D. A.: Towards accurate measurements of soil organic carbon stock change in  
45 agroecosystems, *Can. J. Soil. Sci.*, 86, 465–471, <https://doi.org/10.4141/S05-106>, 2006.
- 46 Webb, E. K., Pearman, G. I., and Leuning, R.: Correction of flux measurements for density effects due to heat and water  
47 vapour transfer, *Q.J Royal Met. Soc.*, 106, 85–100, <https://doi.org/10.1002/qj.49710644707>, 1980.
- 48 Weiss, M. and Baret, F.: S2toolbox Level 2 Products: Lai, Fapar, Fcover, 2016.
- 49 White, J. W., Hunt, L. A., Boote, K. J., Jones, J. W., Koo, J., Kim, S., Porter, C. H., Wilkens, P. W., and Hoogenboom, G.:  
50 Integrated description of agricultural field experiments and production: The ICASA Version 2.0 data standards, *Computers  
51 and Electronics in Agriculture*, 96, 1–12, <https://doi.org/10.1016/j.compag.2013.04.003>, 2013.
- 52  
53  
54